

Humanoid Trajectory Planning for Robot Based on Minimum-Jerk Model of Human Arm

Chengyun Wang

Faculty of Materials and Manufacturing
Beijing University of Technology
Beijing, China
18863501291@163.com

Jing Zhao

Faculty of Materials and Manufacturing
Beijing University of Technology
Beijing, China
zhaojing@bjut.edu.cn

Abstract—In this paper, a humanoid motion planning method for robot trajectory is proposed in this paper. The pick-up and delivery motion in human-robot interaction is firstly studied, and the relationship between the peak velocity and the motion distance in the reaching point motion of the human arm is extracted. Then, based on the minimum-jerk model, a new method to estimate reaching duration is established. The algorithm can more accurately estimate the human arm's motion duration. Finally, the motion law of the human arm is applied to the humanoid trajectory planning of robots. The results show that the humanoid trajectory planning method can effectively improve the quality of human-robot interaction.

Keywords—trajectory planning, human-robot interaction, minimum-jerk model, reaching point motion

I. INTRODUCTION

In human-robot interaction, robots perform tasks according to human motion rules, which is beneficial to human understanding and prediction of robot behavior [1-2]. Therefore, applying the law of human arm motion to the robot in human-robot interaction will improve the quality of human-robot interaction [3].

In the past few decades, scholars have conducted various studies on the motion law of human arm reach point and put forward various models to express the trajectory of human arm end. For example, minimum-jerk model [4], minimum torque model [5], and so on. These results show that the trajectory of the end of the human arm follows a roughly straight path and symmetric bell-shaped velocity waveform, which is the invariable feature of the reaching point motion of the human arm. In order to more accurately express the motion law of the human arm, Kittaka M [6] proposed to express the motion speed of the human arm with the time base generator model given the asymmetric waveform of the motion speed of the human arm. The model focuses on analyzing the difference of individual velocity waveforms. Most of these studies focus on single motion characteristics of human arm motion, such as duration of reaching point motion, average velocity, and peak velocity [7-8]. However, the relationship between peak velocity and reaching point distance is not studied. This is useful for improving the degree of humanoid motion of the robot.

The human-robot interaction process is divided into non-contact human-robot interaction and physical human-robot interaction. Non-contact human-robot interaction focuses on how robots imitate human beings to complete object handover tasks. Non-contact human-robot interaction prepares for human-robot collaboration to complete tasks. In this paper, the contactless human-robot interaction is deeply studied. We

design two experiments of human arm pick-up motion and delivery motion and study the relationship between peak velocity and motion distance when the human arm completes these two motions. A new method for estimating the motion duration to reaching point is proposed based on the minimum-jerk model and the relationship between peak velocity and distance, which makes up for the uncertainty of the motion duration in the minimum-jerk model. The method is compared with Fitts' Law to estimate the motion duration. The results show that the proposed motion duration estimation algorithm is more accurate and stable. Finally, the motion law of the human arm is applied to the end trajectory of robotic arms.

II. MATERIALS AND METHODS

A. Participants

A total of 21 volunteers were recruited to participate in the arms reaching point motion experiment. Eleven volunteers participated in the pick-up motion experiment, and ten volunteers participated in the delivery motion experiment. The volunteers ranged from 24 to 30 and in height from 165 cm to 190 cm. All volunteers were right-handed, had normal hearing and corrected-to-normal vision, and had no history of injuries to their hands, mental illness, or physical disabilities.

B. Data Collection of Reaching Point Motion Experiment

Fig. 1 (a) shows the pick-up motion scene, and the distribution of target points is shown in Fig. 1 (b). There are 108 target points in total, and the distance between adjacent points is 10 cm. These target points constitute the human arm reaching point motion space. The center of the reach space is roughly aligned with the participant's shoulder. The participant's right arm was in a natural droop. Each participant was asked to complete the reaching motion at the speed and comfortable rhythm of daily life. At the end of the motion, the fingertips of the right-hand point to the marked point in Fig. 1 (a). Each marker was repeated three times for a total of 3240 experiments.

The delivery motion experiment scenario is shown in Fig. 2 (a). The delivery motion experiment has ten starting position points and fifteen target position points, the distance between adjacent points is 10 cm, as shown in Fig. 2 (b). Participants placed their hands naturally at the starting point during the experiment and moved to the target point at a natural and comfortable speed. Each marker was repeated three times for a total of 4950 experiments.

In both experiments, the initial and target points were located in the human arm-accessible workspace. During the experiment, each participant wore motion-capture clothes, as shown in Fig.1(a) and Fig. 2(a). The motion capture system

This work is supported by the National Natural Science Foundation of China (No. 51975008).

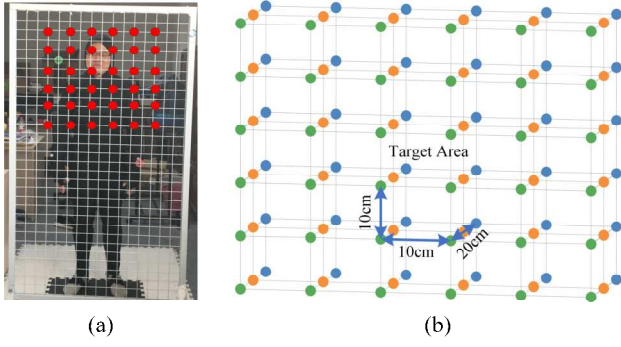


Fig. 1 The pick-up motion experimental scene and target point distribution are shown in (a) and (b), respectively.

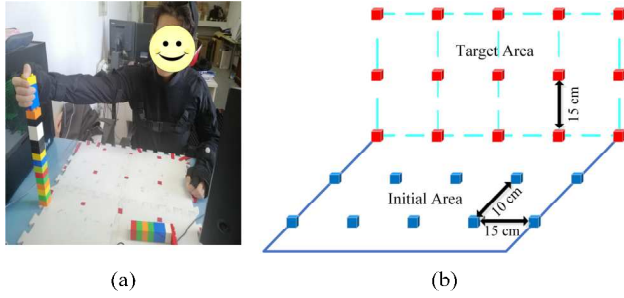


Fig. 2 The delivery motion experiment scene and the distribution of starting and target points are shown in (a) and (b), respectively.

collects the angle values of each arm joint during each participant's reaching point motion at a rate of 120 Hz.

III. ANALYSIS OF THE RELATIONSHIP BETWEEN PEAK VELOCITY AND DISTANCE OF REACH POINT

A. Data Fitting of the Relationship between Peak Velocity and Reaching Point Distance

The variation law of peak velocity with the distance to the reaching point was analyzed when the human arm completed the pick-up and delivery motion, and the scatter diagram of peak velocity varying with the distance to the reaching point was obtained, as shown in Fig. 3.

It can be seen from Fig. 3(a) and (b) that the peak value of reaching point velocity increases with the increase of reaching point distance, and there is an obvious linear relationship between the peak value of reaching point velocity and reaching point distance. However, the fluctuation range of the

original data is large, and the error of the peak value of the point velocity estimated by the function relationship obtained by data fitting is significant. In order to improve the estimation accuracy of the peak velocity of the reaching point, the average value of the peak velocity within each interval of the reaching point distance was obtained with 1 mm interval, which was used as the peak velocity of the reaching point distance. For example, take the average value of velocity peak values of all experimental data between 100 mm and 101 mm, and the average velocity peak value obtained at this time is the corresponding velocity peak value when the distance is 101mm. The calculation formula is as follows:

$$V_i = \sum_{j=1}^n V_{ij} / n \quad (1)$$

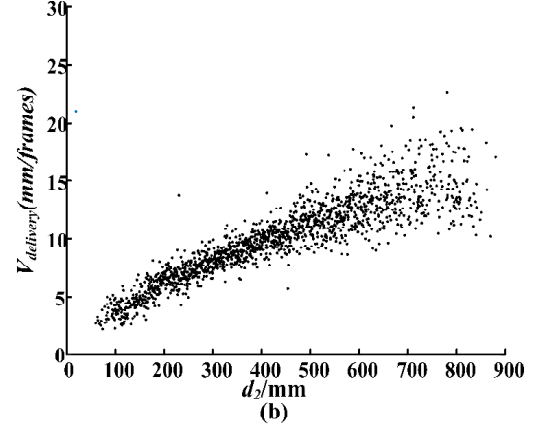
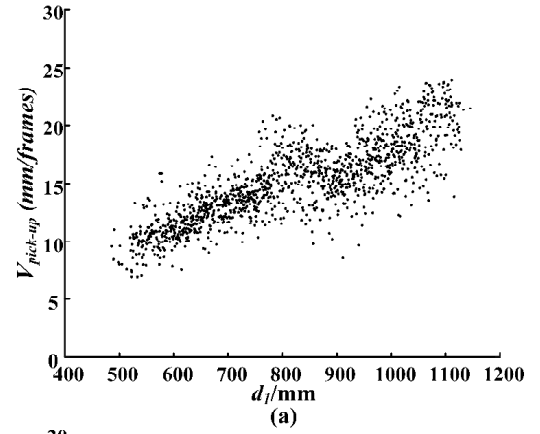


Fig. 3 Scatter diagrams of velocity peak value and reaching point distance in the pick-up motion and delivery motion are in (a) and (b), respectively.

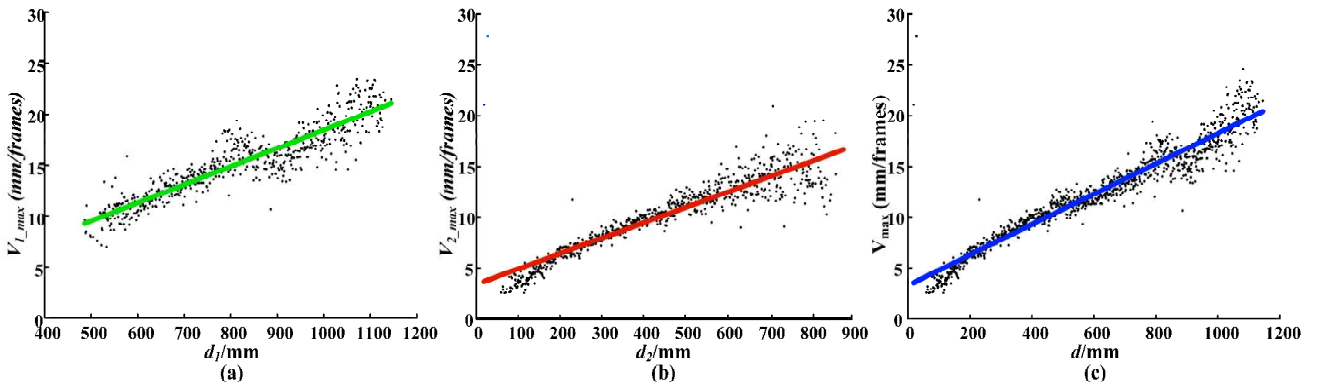


Fig. 4 The fitting curves between the velocity peak value and the reaching point distance are in (a) (b), respectively. The fitting curve of all data of pick-up and delivery motion is in (c).

Where, V_i is the peak of reaching point velocity when the reaching point distance is i mm. n is the number of experimental data when the distance of reaching point is between $i-1$ and i mm. V_{ij} is the velocity peak of the j -th experimental data when the distance to the point is between $i-1$ and i mm.

The experimental data of motion pick-up and delivery are processed by formula (1), and the results are shown in Fig. 4. After data processing, the linear relationship between peak velocity and reaching point distance is more obvious. It can be seen from Fig. 4 that the relationship between peak velocity and reaching point distance is consistent in pick-up and delivery motion.

In order to formalize the relationship between peak velocity and reaching point distance, experimental data were fitted. In the pick-up motion, the fitting function between the peak velocity and the reaching point distance is:

$$V_{p_max} = 0.0179 \times d_p + 0.8202 \quad (2)$$

Where, V_{p_max} is the pick-up motion reaching point velocity peak. d_p is the reaching point distance of pick-up motion, that is, the straight-line distance between the starting point and the target point. The goodness of fit R^2 is 0.9032.

In the delivery motion, the fitting function between the peak velocity and the reaching point distance is:

$$V_{d_max} = 0.0150 \times d_d + 3.4300 \quad (3)$$

Where, V_{d_max} is the delivery motion reaching point velocity peak. d_d is the reaching point distance of the delivery motion, that is, the straight-line distance between the starting point and the target point. The goodness of fit R^2 is 0.9194.

Data fitting was carried out together with the reaching point experimental data of pick-up motion and delivery motion, and the fitting results were shown in Fig. 5(c). At this point, the fitting function between the peak point velocity and the reaching point distance is:

$$V_{max} = 0.0149 \times d + 3.3143 \quad (4)$$

Where, V_{max} is the reaching point velocity peak. d is the reaching point distance, that is, the straight-line distance between the starting point and the target point. The goodness of fit R^2 is 0.9704.

B. Analysis of the Influence of Different Starting Points on The Relationship Between Peak Velocity and Reaching Point Distance

In order to study whether the relationship between peak velocity and reaching point distance is significantly affected by the motion of reach point from different starting points. Data fitting was carried out for the relationship between the peak velocity value and the reaching point distance from different starting points. The results are shown in Table 1.

It can be seen from Table 1 that the fitting parameter p1 of the fitting curve between the peak velocity and reaching point distance changes within the interval [0.0143, 0.0197] when the reaching point motion is carried out from different starting points. The difference of parameter p1 is 0.0054. The parameter p2 varies within the interval [0.5574, 3.9835]. The

TABLE I. FITTING PARAMETERS OF PEAK VELOCITY AND REACHING POINT DISTANCE AT DIFFERENT STARTING POINTS

Start Point	p1	p2	R ²
1	0.0154	2.8861	0.9112
2	0.0162	2.7449	0.8403
3	0.0195	1.3702	0.9687
4	0.0190	2.1517	0.9750
5	0.0146	3.9457	0.9811
6	0.0155	3.1401	0.9996
7	0.0177	3.1240	0.9946
8	0.0197	2.6427	0.9440
9	0.0148	3.9265	0.8147
10	0.0143	3.9835	0.9551
11	0.0179	0.5574	0.9032
All	0.0149	3.3143	0.9704

difference of parameter p2 is 3.4261. The parameters P1 and P2 vary within a small range. The fitting goodness R^2 changed within the interval [0.8147, 0.9996]. As seen from the above analysis, the curve fitting effect of function between peak velocity and reaching point distance is better when the reaching point motion is carried out from different starting positions.

The sample data of the reaching point motion from the same starting point were formed into a group of data, and 11 groups of experimental data were obtained. A variance test was carried out on these 11 groups of data to verify whether the relationship between peak velocity and reaching point distance is significantly affected by the completion of reaching point motion from different starting points. The variance test is $F_{actual} = 1.06 < F_{check} = 4.84$, $P = 0.4172 > 0.05$.

The results of the variance test show that the motion from different starting points has no significant influence on the relationship between peak velocity and distance. In other words, the function relationship between peak velocity and reaching point distance at different starting points is similar.

C. Analysis of the Influence of Different Participants on Peak Velocity and Distance Curve

In order to study whether the relationship between peak velocity and reaching point distance of different participants is significantly different, data fitting is performed on the relationship between peak velocity and reaching point distance of each participant. The results of pick-up motion and delivery motion are shown in Table II and Table III, respectively.

It can be seen from Table II that in the pick-up motion, the data fitting parameter p1 of the function curve between the speed peak and the reaching point distance varies within the interval [0.0097, 0.224]. The maximum difference of parameter p1 is 0.2143. The parameter p2 varies within the interval [-0.4936, 5.0201]. The maximum difference of parameter p2 is 5.5137. The variance test was conducted on the motion data of the 10 participants in the pick-up motion, and the variance test result was $F_{actual} = 83.19 > F_{check} = 4.96$. In other words, the functional relationship between the peak velocity and the reaching point distance between different participants has a significant difference in the pick-up motion.

It can be seen from Table III that in the delivery motion, the data fitting parameter p1 of the function curve between the speed peak and the reaching point distance varies within the

TABLE II. SPEED PEAK VALUES AND DISTANCE FITTING PARAMETERS OF DIFFERENT PARTICIPANTS IN THE PICK-UP MOTION

Participant	p1	p2	R ²
1	0.0196	-0.4936	0.9291
2	0.0197	0.2959	0.9375
3	0.0121	3.9758	0.8091
4	0.0224	1.1855	0.9025
5	0.0101	5.0201	0.9934
6	0.0140	4.7482	0.8487
7	0.0139	4.0633	0.9577
8	0.0097	3.3302	0.9796
9	0.0141	2.3345	0.8351
10	0.0170	1.7925	0.8547
11			
All	0.0179	0.5574	0.9032

TABLE III. SPEED PEAK VALUES AND DISTANCE FITTING PARAMETERS OF DIFFERENT PARTICIPANTS IN THE DELIVERY MOTION

Participant	p1	p2	R ²
1	0.0172	4.7888	0.8750
2	0.0127	2.2991	0.9358
3	0.0147	4.6499	0.9876
4	0.0094	6.0498	0.5801
5	0.0210	1.8174	0.9645
6	0.0179	2.4209	0.9518
7	0.0119	4.1386	0.8846
8	0.0205	2.6717	0.8696
9	0.0125	4.5784	0.9258
10	0.0158	1.6958	0.9260
11	0.0186	2.9254	0.9154
All	0.0150	3.4300	0.9194

interval [0.0094,0.210]. The maximum difference of parameter p1 is 0.2006. The parameter p2 varies within the interval [1.6958,6.0498]. The maximum difference of parameter p2 is 4.3540. The variance test was conducted on the motion data of the 11 participants in the delivery motion, and the variance test result was $F_{actual}=20.96 > F_{check}=4.84$. In other words, the functional relationship between the peak velocity and the reaching point distance between different participants has a significant difference in the delivery motion.

To sum up, it can be seen that there is a certain difference between the velocity peak and the reaching point distance function of different participants' reaching point motion, but the difference is within an acceptable range.

IV. ESTIMATE THE MOTION DURATION OF THE HUMAN ARM

A. Estimation Algorithm of Reaching Point Motion Duration of the Human Arm

Hand trajectory during a proficient reaching motion follows a roughly straight path with a symmetrical bell-shaped velocity profile, which are the invariant features of reaching motions. Therefore, the minimum-jerk model is used to express the motion state of the end trajectory of the human arm. The end velocity of the human arm in reaching point motion can be expressed as[4]:

$$\dot{P}(t) = (P_0 - P_f)(60\tau^3 - 30\tau^4 - 30\tau^2) / T_p \quad (5)$$

Where $\dot{P}(t)$ is the derivatives of $P(t)$. It can be obtained by integrating equation (5). T_p is the duration of motion of the end of the human arm. P_0 , P_f is the starting point and target point position, respectively. Moreover, $\tau = t/T_p$, $t \in [0, T_p]$.

According to equation (5), the minimum-jerk model is a function of the end velocity of the human arm with respect to duration, starting position, and target position. In this function, the position of starting point and target point is known, while the motion duration of the reaching point of the human arm is unknown. Therefore, it is necessary to estimate the duration of the human arm to express the trajectory of the end of the arm fully. Since the minimum-jerk model is the symmetric function, when $t = T_p/2$, the speed of the minimum-jerk model reaches the maximum. According to equation (4), it can be seen that there is a linear relationship between the peak velocity of the reaching point motion and the distance of the reaching point. Therefore, the arm motion duration T_p of the reaching point motion can be obtained from (4) and (5).

$$T_p = -1.875\delta \|P_0 - P_f\|_2 / (0.0149d + 3.3143) \quad (6)$$

Where, $\delta = -1$, P_0 , P_f is the starting point and target point position, respectively.

B. Comparison of Estimation Methods of Reaching Point Motion Duration of the Human Arm

In order to verify the accuracy of the proposed algorithm, the proposed algorithm was used to estimate the motion duration of the experimental sample, and the comparison was made with the motion duration of the experimental sample estimated by Fitts' law.

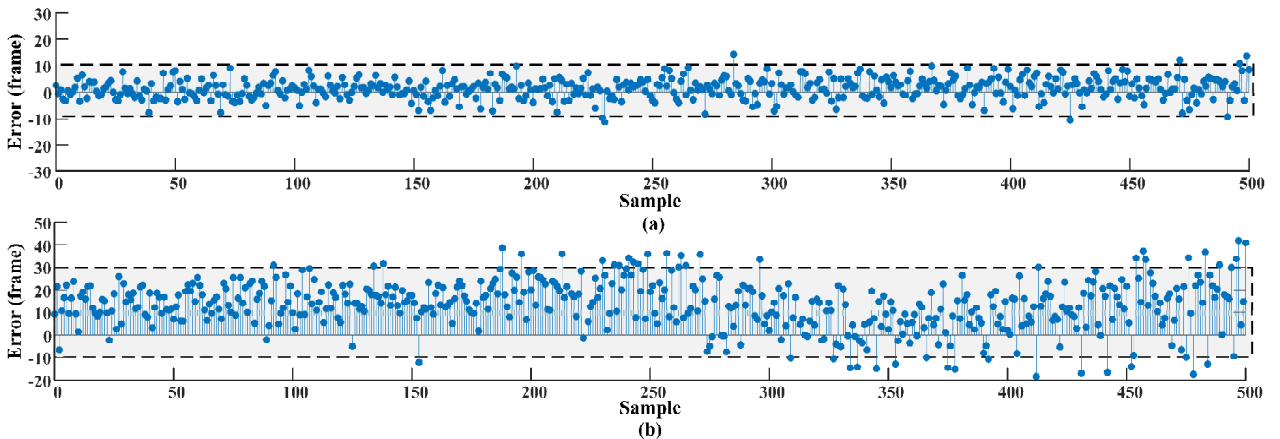


Fig. 5 The duration estimation error. The duration estimation errors of this paper and Fitts' Law are in (a) and (b), respectively. 1 s is 120 frames.

Fitts' Law for estimating the motion duration T_F of the human arm is[9]:

$$T_F = a + b \log_2(2A/W) \quad (7)$$

where A is the Euclidean distance between the starting point and the target point, and W is the size of the target. Based on the experimental device in Fig. 1 and Fig. 2, W is set to 20 mm. a and b are undetermined coefficients. According to the experimental data of section II B, the values of a and b are obtained by the regression method. They are $a=0.3625$ and $b=0.1325$, respectively.

Two-duration estimation methods were used to estimate the duration of 500 randomly selected experimental samples, and the error between the estimated value and the actual value of each sample was calculated, as shown in Fig. 5. As can be seen from the figure, the duration estimation error of the proposed duration estimation algorithm is less than 10 frames, and the standard deviation is 3.9154. Fitts' Law's duration estimation error mainly varies from -10 frames to 30 frames, and the standard deviation is 11.4418. It can be seen that the time estimation algorithm proposed in this paper has not only minor errors but also stable errors.

V. THE HUMANOID EXPERIMENT OF ROBOT TERMINAL TRAJECTORY

The proposed duration estimation method and Fitts' Law duration estimation method combined with the minimum-jerk model are used to plan the terminal trajectory of IIWA robot respectively to realize the humanoid motion of the robot. The experimental process is compared with the human arm reaching-point motion process, as shown in Fig. 6.

Participants wore motion capture clothing to complete the reaching point motion from the marked starting point to the target point. The motion capture system recorded the data of human arm motion at a frequency of 120HZ. The two humanoid trajectory planning methods' starting pose and target pose are the same. The distance from the starting point of the robot to the target point is roughly the same as the distance of the human arm reaching point motion. The starting

position P_s , pose O_s and swivel angle Φ_s of the robot are respectively:

$$P_s = [-0.5157, 0.2078, 0.3540]$$

$$O_s = [67.36, -60.01, 17.24]$$

$$\Phi_s = 88.0804$$

The ending position P_f , pose O_f and swivel angle Φ_f of the robot are respectively:

$$P_f = [0.5668, 0.6083, 0.7479]$$

$$O_f = [-62.35, 34.45, 173.75]$$

$$\Phi_f = 91.9196$$

The humanoid trajectory of redundant robot arm pose is obtained by the method in [10]. The trajectory of the robot's swivel angle $\Phi(t)$ and pose $O(t)$ obtained are respectively:

$$\dot{\Phi}(t) = \frac{A_\Phi}{2} \left(1 - \cos\left(\frac{2\pi t}{T_\Phi}\right) \right) \quad (8)$$

$$\dot{O}(t) = \frac{A_O}{2} \left(1 - \cos\left(\frac{2\pi t}{T_O}\right) \right) \quad (9)$$

where $\dot{\Phi}(t)$, $\dot{O}(t)$ are the derivatives of $\Phi(t)$, and $O(t)$, respectively. T_Φ , and T_O are the duration of the Φ , and O , respectively. $A_\Phi = 2(\Phi_f - \Phi_0)/T_\Phi$, Φ_0 and Φ_f are the initial and end values of Φ , respectively. $A_O = 2(O_f - O_0)/T_O$, O_0 and O_f are the initial and end values of O , respectively.

Finally, according to the analytical method in [11], the robot terminal position $P(t)$, pose $O(t)$ and swivel angle $\Phi(t)$ are converted into the robot joint angle.

It can be seen from Fig. 6 that the humanoid trajectory planning method proposed in this paper makes the motion duration of the robot close to the motion duration of the human arm with a difference of about 0.07s for the same reaching point motion distance. However, the humanoid trajectory planning method based on Fitts' Law makes the robot move

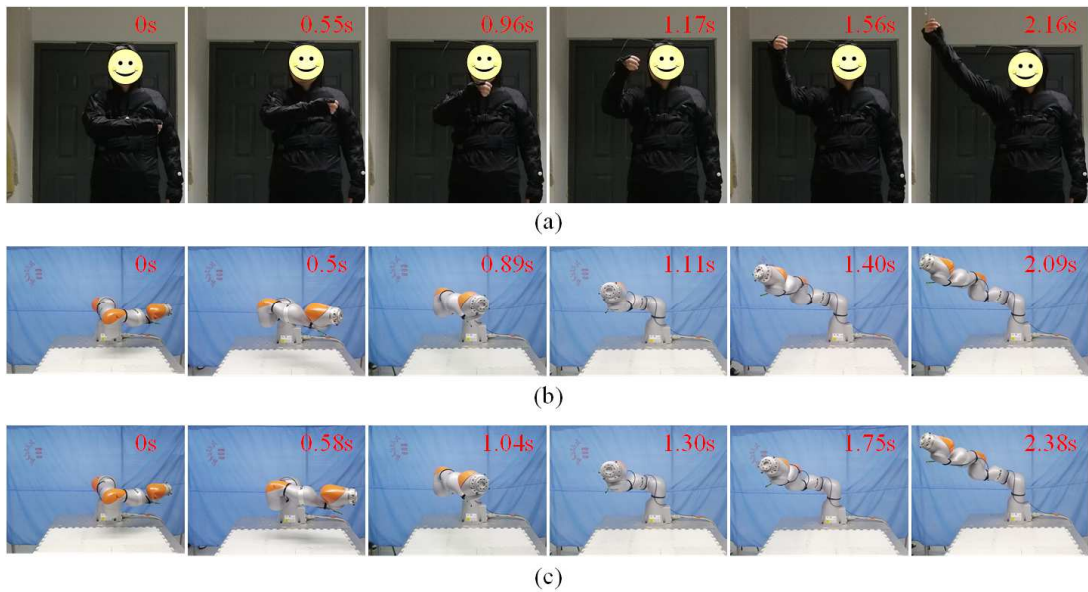


Fig. 6 Snapshots of the reaching point motion experiment. (a) Human arm reach pointing experiment. (b) Robot reaching motion experiment with the proposed duration estimation method. (c) Fitts' Law estimation of duration for robot reaching motion experiment.

for a long time, which is 0.22s slower than the human arm to complete the same reaching point distance.

VI. CONCLUSION

In this paper, the relationship between the peak velocity of the human arm and the distance of the human arm reaching point is studied. The linear function between the peak velocity and the reaching point distance is determined and verified. On this basis, a new method for estimating the time of reaching point motion of the human arm is proposed by combining the minimum-jerk model. This method is more accurate than Fitts' Law duration estimation method. Finally, it is applied to IIWA robot trajectory humanoid motion planning, which makes the robot motion have high humanoid and improves the acceptability of the robot in human-robot interaction.

References

- [1] K. Chang, J. Gao, B. Liu, J. Yin, M. Yan and G. Zhang, "Design and Implementation of Grinding Robot Control System for Circumferential Weld on Inner Wall of Pipe," 2021 6th International Conference on Automation, Control and Robotics Engineering (CACRE), pp. 11-15, 2021.
- [2] Jing Zhao, Chengyun Wang, et al., "Motion pattern of human arm reaching point movements based on the movement primitives," *Journal of Mechanical Engineering*, vol. 57, no. 19, pp. 1-8, 2021.
- [3] Yun, S., "A gaze control of socially interactive robots in multiple-person interaction," *Robotica*, vol. 35, no. 11, pp. 2122-2138, 2017.
- [4] Viviani, et al., "Minimum-jerk, two-thirds power law, and isochrony: Converging approaches to movement planning," *Journal of Experimental Psychology*, vol. 1, no. 2, pp. 300-310, 1995.
- [5] Uno, Y., M. Kawato, and R. Suzuki, "Formation and control of optimal trajectory in human multijoint arm movement," *Biological Cybernetics*, vol. 61, no. 2, pp: 89-101, 1989.
- [6] Kittaka M, Furui A, Sakai H, et al., "Spatiotemporal Parameterization of Human Reaching Movements Based on Time Base Generator," *IEEE Access*, vol.1, no. 1, pp. 199-206, 2020.
- [7] E. Jaspers, K. Desloovere, H. Bruyninckx, G. Molenaers, K. Klingels, and H. Feys, "Review of quantitative measurements of upper limb movements in hemiplegic cerebral palsy," *Gait Posture*, vol. 30, no. 4, pp. 395-404, 2009.
- [8] A. De Los Reyes-Guzmán, I. Dimbwadjo-Terrer, F. Trincado-Alonso, F. Monasterio-Huelin, D. Torricelli, and A. Gil-Agudo, "Quantitative assessment based on kinematic measures of functional impairments during upper extremity movements: A review," *Clin. Biomech*, vol. 29, no. 7, pp. 719-727, 2014.
- [9] Mackenzie, I. Scott, "Fitts' Law as a Research and Design Tool in Human-Computer Interaction," *Human-Computer Interaction*, vol 7, no 1, pp.120-126, 1992.
- [10] Shiqiu Gong, Jing Zhao, "Robot Motion Planning with Human-Like Motion Patterns based on Human Arm Movement Primitive Chains," in *2021 IEEE International Conference on Robotics and Automation (ICRA)*, Xian, pp. 6281-6288, 2021.
- [11] Gong, S., Zhao, J., Zhang, Z. and Xie, B., "Task motion planning for anthropomorphic arms based on human arm movement primitives," *Industrial Robot*, vol. 4, no. 5, pp. 669-681, 2020.